

Monte Carlo calculations of the hydrostatic compression of hexahydro-1,3,5-trinitro-1,3,5-triazine and β -octahydro-1,3,5,7-tetranitro-1,3,5,7-tetrazocine

Thomas D. Sewell^{a)}

Theoretical Division, Los Alamos National Laboratory, Los Alamos, New Mexico 87545

(Received 17 November 1997; accepted for publication 14 January 1998)

Rigid molecule Monte Carlo simulations are used in a computational study of the isothermal, hydrostatic compression of crystalline hexahydro-1,3,5-trinitro-1,3,5-triazine and β -octahydro-1,3,5,7-tetranitro-1,3,5,7-tetrazocine for pressures in the range $0 \text{ GPa} \leq p \leq 7.5 \text{ GPa}$. The purpose of the investigation is to assess the utility of simple intermolecular potential-energy functions, generally parameterized for ambient conditions of temperature and pressure, for studies of polyatomic molecular crystals under the extremes of pressure that are important in accident scenarios involving high explosives. The calculated results are found to be in good agreement with published x-ray diffraction data. © 1998 American Institute of Physics. [S0021-8979(98)05608-4]

I. INTRODUCTION

Under the provisions of the Comprehensive Test Ban Treaty,¹ testing of nuclear weapon systems is forbidden. Thus, it is necessary to certify the safety, performance, and reliability of the enduring nuclear stockpile on the basis of computational physics, augmented by state-of-the-art non-nuclear experiments. Since high explosives are important components in both nuclear and conventional weapon systems, we must develop a thorough understanding and reliable predictive capability of the physics of these complicated materials over wide domains of pressure, temperature, and strain rate. Among the quantities of interest in this connection are crystal lattice parameters, density, coefficients of thermal and baric expansion, specific heats, transport coefficients, mechanical properties, and chemical kinetics. Experimental data for these quantities are either sparse or nonexistent for the materials of interest,² yet they are needed for the construction and/or calibration of new micromechanical physics models to be implemented in larger-scale modeling codes.

In this article we report Monte Carlo calculations of the physical properties of two widely used high explosives, hexahydro-1,3,5-trinitro-1,3,5-triazine (RDX) and β -octahydro-1,3,5,7-tetranitro-1,3,5,7-tetrazocine (β -HMX), under hydrostatic compression. We focus on the crystalline state and isothermal conditions, and restrict the discussion to properties for which comparisons can be made to experimental data.

II. METHODS

A. Theoretical approach

Our approach is statistical mechanical, employing the numerical technique of classical Monte Carlo, whereby the thermophysical properties follow from the interaction potential U_N . Specifically, in isothermal-isobaric Monte Carlo³

the macroscopic property $A(N, p, T)$ of a system of N rigid molecules at temperature T and scalar pressure p is obtained as an average of the microscopic function of configuration $A(\mathbf{q}, \Theta; V)$, where \mathbf{q} and Θ denote molecular positions and orientations, respectively, and V is the volume of the simulation cell. The average is taken over the states of a Markov chain in the configuration space of the system,

$$A(N, p, T) = \lim_{M \rightarrow \infty} \frac{1}{M} \sum_{m=1}^M A(\mathbf{q}_m, \Theta_m; V_m), \quad (1)$$

in which the transition matrix between successive states is based on the potential energies $U_N(\mathbf{q}_m, \Theta_m)$ in such a way as to assure detail balance and the equality of $A(N, p, T)$ with the actual ensemble average in the isothermal-isobaric ensemble,

$$\langle A_{NpT} \rangle = \frac{\int dV e^{-\beta p V} \int d\mathbf{q} \int d\Theta A(\mathbf{q}, \Theta; V) e^{-\beta U_N(\mathbf{q}, \Theta)}}{\int dV e^{-\beta p V} \int d\mathbf{q} \int d\Theta e^{-\beta U_N(\mathbf{q}, \Theta)}}, \quad (2)$$

where $\beta = 1/\kappa T$.

In isothermal-isobaric Monte Carlo, it is most convenient to express the molecular positions in terms of scaled coordinates $\mathbf{s} = \tilde{\mathbf{h}}^{-1} \mathbf{q}$, where $\tilde{\mathbf{h}}$ is the matrix which transforms between the two coordinate systems. The columns of $\tilde{\mathbf{h}}$ are the lattice vectors \mathbf{a} , \mathbf{b} , and \mathbf{c} . For the cubic volumes normally used in isothermal-isobaric simulations of liquids, the elements of $\tilde{\mathbf{h}}$ are just $h_{ij} = V^{1/3} \delta_{ij}$.³ However, for studies of solids, one needs to allow for changes in both the volume and shape of the simulation cell. In this case, $\tilde{\mathbf{h}}$ is an upper triangular matrix, i.e., there are six independent variables that specify the size and shape of the simulation cell. This generalization has been described in detail by Parrinello and Rahman⁴ for molecular dynamics simulations, and by Yas-honath and Rao⁵ for Monte Carlo calculations of atomic solids.

Recasting the integral in terms of these dimensionless coordinates and noting that $d\mathbf{q}_k = \|\tilde{\mathbf{h}}\| d\mathbf{s}_k = V(\tilde{\mathbf{h}}) d\mathbf{s}_k$ yields

^{a)}Electronic mail: sewell@lanl.gov

TABLE I. Repulsion and dispersion parameters used in Eq. (5).^{a,b}

<i>i</i>	<i>a</i> (kJ ^{1/2} mol ^{-1/2})	<i>b</i> (Å ⁻¹)	<i>c</i> (kJ ^{1/2} mol ^{-1/2} Å ³)
C ^c	608.065	1.80	49.394
H ^c	109.411	1.87	11.678
N ^c	504.509	1.89	37.127
O ^d	479.655	1.98	33.601

^aFor the potential designated DEW. Parameters for the SRT potential are provided in Ref. 9.

^b $A_{ij}=a_i a_j$; $B_{ij}=b_i + b_j$; $C_{ij}=c_i c_j$.

^cReference 6.

^dReference 7.

$$\langle A_{NpT} \rangle$$

$$= \frac{\int d\tilde{\mathbf{h}} \int d\mathbf{s} \int d\mathbf{\Theta} A(\mathbf{s}, \mathbf{\Theta}; V(\tilde{\mathbf{h}})) e^{-\beta[U_N(\mathbf{s}, \mathbf{\Theta}) + pV(\tilde{\mathbf{h}}) - (N/\beta) \ln V(\tilde{\mathbf{h}})]}}{\int d\tilde{\mathbf{h}} \int d\mathbf{s} \int d\mathbf{\Theta} e^{-\beta[U_N(\mathbf{s}, \mathbf{\Theta}) + pV(\tilde{\mathbf{h}}) - (N/\beta) \ln V(\tilde{\mathbf{h}})]}}. \quad (3)$$

Thus the average is an integral spanning the $6N$ coordinates of the molecular positions and orientations contained in a unit cube plus six additional degrees of freedom corresponding to independent variations of the elements of $\tilde{\mathbf{h}}$.

B. Potential-energy surface

The intermolecular potentials are of the form

$$U(\mathbf{R}) = \sum_A \sum_{B>A} \sum_{i \in A} \sum_{j \in B} [U_{rep}(\mathbf{R}_{ij}) + U_{disp}(\mathbf{R}_{ij}) + U_{elec}(\mathbf{R}_{ij})], \quad (4)$$

where A and B are molecules, and i and j denote particular atoms. The repulsion, dispersion, and electrostatic terms are written as

$$\begin{aligned} U_{rep} &= A_{ij} e^{-B_{ij} R_{ij}}, \\ U_{disp} &= -C_{ij} / R_{ij}^6, \\ U_{elec} &= q_i q_j / R_{ij}. \end{aligned} \quad (5)$$

The parameters A , B , and C were taken from the work of Williams and co-workers^{6,7} and are collected in Table I. Potential derived atomic charges were calculated using the CHELPG method within the Gaussian 92 suite of programs,⁸ at the HF/6-31g* level of theory, for the experimentally determined geometries of the molecules in the crystal. These are presented in Table II. After the work described here was substantially completed, Sorescu, Rice, and Thompson⁹ reported a set of potential parameters for the same functional form used by Williams (and, in fact, based largely on the Williams parameterization) but optimized specifically for RDX under ambient conditions. Therefore, we include representative calculations for the latter parameter set. Note, however, that we use the same charges, calculated in the manner described above, in all the computations reported below.

TABLE II. Calculated partial charges for RDX and β -HMX.

RDX		β -HMX	
Atom designation ^a	Partial charge (<i>e</i>)	Atom designation ^b	Partial charge (<i>e</i>)
C(1)	-0.106 620	N(1)	0.756 035
C(2)	-0.064 523	N(2)	-0.050 655
C(3)	-0.081 264	N(3)	0.155 701
N(1)	0.094 755	N(4)	0.702 034
N(2)	-0.316 284	O(1)	-0.436 423
N(3)	-0.328 492	O(2)	-0.429 558
N(4)	0.613 940	O(3)	-0.439 181
N(5)	0.859 409	O(4)	-0.395 792
N(6)	0.868 195	C(1)	-0.258 530
O(1)	-0.400 242	C(2)	-0.384 209
O(2)	-0.422 452	H(1)	0.165 480
O(3)	-0.423 644	H(2)	0.184 699
O(4)	-0.442 078	H(3)	0.215 097
O(5)	-0.418 378	H(4)	0.215 684
O(6)	-0.446 095	N(5)	0.762 890
H(1)	0.141 281	N(6)	-0.044 989
H(2)	0.193 003	N(7)	0.166 785
H(3)	0.194 909	N(8)	0.703 571
H(4)	0.170 866	O(5)	-0.437 177
H(5)	0.129 017	O(6)	-0.431 915
H(6)	0.184 700	O(7)	-0.440 872
		O(8)	-0.395 126
		C(3)	-0.308 706
		C(4)	-0.378 961
		H(5)	0.179 789
		H(6)	0.197 940
		H(7)	0.212 583
		H(8)	0.213 805

^aAs defined in Ref. 13.

^bAs defined in Ref. 15 for atoms N(1)–H(4). Atoms N(5)–H(8) are obtained by the inversion operation on atoms N(1)–H(4), respectively, in fractional coordinates.

C. Computational details

We consider perfectly rigid molecules. Thus, three kinds of trial moves are necessary to explore the configuration space of the system: translations of the molecular centers of mass, rotations of the molecules about their centers of mass, and changes in the size and shape of the simulation cell. Molecular translations and rotations were performed using the algorithm of Barker and Watts,¹⁰ adapted for use with scaled coordinates. The Markov chain was generated using a Metropolis¹¹ algorithm in which trial moves are accepted with probability $P = \min[\exp(-\Delta), 1]$, where, for present state m and “trial” state $m+1$,

$$\begin{aligned} \Delta &= \beta \{ [U_N^{m+1} - U_N^m] + p[V^{m+1} - V^m] \} \\ &\quad - N \ln(V^{m+1}/V^m). \end{aligned} \quad (6)$$

Maximum displacements were adjusted to yield roughly a 50% acceptance probability for a given kind of move. The battery of analyses described by Hald¹² was used to assess whether a particular Monte Carlo realization was under statistical control. Uncertainties reported below correspond to the standard error of the mean, obtained from statistically independent subaverages computed along the Markov chain.

The bulk crystal was simulated by periodic replication in three dimensions of a primary simulation cell containing N

TABLE III. Calculated lattice lengths and unit cell volume for RDX. Uncertainties in the last reported digit are included in parentheses. Only results for the potential parameters of Williams and co-workers (Refs. 6 and 7) are included.

Pressure (GPa)	Lattice lengths (Å)			Unit cell volume (Å ³)
	<i>a</i>	<i>b</i>	<i>c</i>	
0.00	13.399(5)	11.739(3)	10.789(9)	1696. (1)
0.50	13.278(5)	11.642(3)	10.598(7)	1638. (1)
0.73	13.230(5)	11.600(3)	10.543(8)	1617.3(8)
1.75	13.053(8)	11.418(4)	10.367(9)	1544.4(6)
2.75	12.937(4)	11.275(3)	10.200(8)	1487.2(6)
3.36	12.887(3)	11.219(2)	10.115(3)	1462.0(3)
3.95	12.837(4)	11.179(3)	10.064(3)	1443.9(4)

molecules. The replication was extended far enough into space to account for all potential interactions between molecules having centers of mass separated by 20 Å or less. Primary simulation cells containing from one to 27 copies of the crystallographic unit cell were considered. However, as will be shown, the results are quite insensitive to the size of simulation. In order to allow for comparisons to the experimental data, calculations were performed as a function of pressure for a constant temperature of $T=298$ K.

III. RESULTS AND DISCUSSION

The calculated results for RDX and β -HMX are collected in Tables III and IV, respectively. The densities computed at $T=298$ K and $p=0.0$ GPa are 3.6% and 5.4% lower than the experimental values for RDX and β -HMX, respectively. This is not surprising since the Williams parameters were obtained by adjusting their values to optimize agreement between experimental crystal structures determined at finite temperatures and theoretical, energy-minimized structures corresponding to $T=0$ K, resulting in atoms that are slightly “too big” when used in calculations where temperature and pressure are explicitly considered.

TABLE IV. Calculated lattice parameters and unit cell volume for β -HMX. Uncertainties in the last reported digit are included in parentheses. Only results for the potential parameters of Williams and co-workers (Refs. 6 and 7) are included.

Pressure (GPa)	Lattice Parameters (Å and deg.)				Unit cell volume (Å ³)
	<i>a</i>	<i>b</i>	<i>c</i>	β	
0.00	6.674(7)	11.17 (1)	8.95 (1)	124.5 (1)	549.3(6)
0.50	6.592(3)	11.044(9)	8.895(7)	125.38(9)	527.3(4)
1.00	6.529(4)	10.964(7)	8.836(7)	125.71(8)	513.1(3)
1.61	6.472(4)	10.885(6)	8.785(6)	126.00(6)	500.2(3)
2.47	6.414(3)	10.807(5)	8.705(6)	126.15(6)	486.9(2)
3.24	6.366(3)	10.745(5)	8.659(6)	126.16(7)	477.8(2)
4.03	6.327(3)	10.690(7)	8.613(5)	126.15(6)	470.1(2)
4.82	6.294(3)	10.643(7)	8.563(6)	126.13(5)	463.1(2)
5.42	6.274(3)	10.610(6)	8.543(5)	126.13(5)	459.1(2)
6.31	6.241(3)	10.567(5)	8.500(5)	126.07(5)	452.9(2)
6.74	6.226(3)	10.547(5)	8.484(3)	126.03(5)	450.3(1)
7.47	6.208(3)	10.509(7)	8.459(5)	126.03(5)	446.1(2)

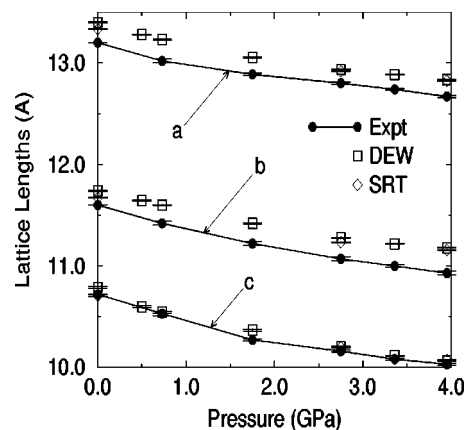


FIG. 1. The calculated lattice lengths *a*, *b*, and *c* for RDX are compared to the experimental values as a function of pressure. Filled circles: experiment; open symbols: calculation. DEW and SRT denote calculations performed using the repulsion and dispersion potential parameters of Williams and co-workers (Refs. 6 and 7) and Sorescu *et al.* (Ref. 9), respectively. Experimental data are taken from Ref. 14. The line segments connecting the experimental data points are only included as a guide for the eye.

A. RDX

At room temperature and pressure, RDX crystallizes in the orthorhombic space group *Pbca*, with $Z=8$ molecules per unit cell.¹³ Olinger *et al.*¹⁴ determined from an x-ray diffraction study of the pressure dependence of the lattice parameters at $T=293$ K that this is the stable space group of RDX for $p < 3.95$ GPa. In Fig. 1 we provide a comparison of the calculated and measured lattice lengths of RDX over that pressure domain. The agreement is quite good; the maximum discrepancy occurs for the length of *a*, but the magnitude of the error is only 1.5% and 2.3% at $p=0$ GPa and 3.95 GPa, respectively. Moreover, the derivatives $\partial X/\partial p|_T$ ($X=a, b, c$) are in better agreement with experiment than are the raw magnitudes. The choice of the potential parameters of Sorescu *et al.* (SRT)⁹ versus those of Williams and co-workers (DEW)^{6,7} has little influence under the conditions considered here. Finally, the mean values for the lattice angles α, β , and γ (not shown) never vary from the orthorhombic value of 90 degrees by more than ± 0.13 degree.

B. β -HMX

HMX exists in four different polymorphic forms. The stable structure under ambient conditions is known as β -HMX, and it crystallizes in the monoclinic space group *P2₁/c*, with $Z=2$ molecules per unit cell.¹⁵ Representative calculations were performed to assess possible finite-size effects that might arise when using a primary simulation cell comprised of so few molecules. Namely, at $T=298$ K, $p=4.03$ GPa, calculations were done for primary simulation cells containing $N=2, 4, 16$, and 54 molecules, and the results plotted versus $1/N$ such that the y intercept of a straight line fit through the data corresponds to the result for an “infinite” system. For all properties reported here, the percent differences in the results for $N=2$ and $N=\infty$ were less than 0.4%. Consequently, we performed the remainder of the calculations using $N=2$.

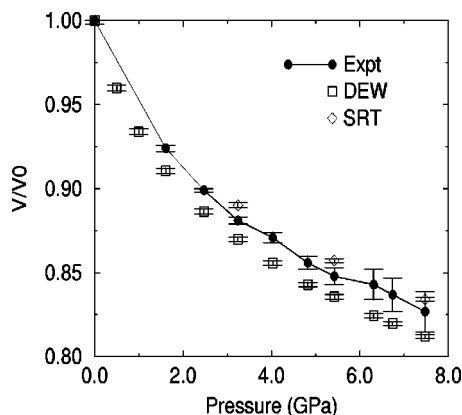


FIG. 2. The same as in Fig. 1 except the calculated volumetric compression of β -HMX is compared to experiment. The quantity V/V^0 is the ratio of the unit cell volume at pressure p to the corresponding value for $p=0$.

Olinger *et al.*¹⁴ determined that, at $T=293$ K, β -HMX is stable for pressures up to $p=7.47$ GPa. Our calculations yield good agreement with their data, although not to the same degree as was the case for RDX. The trends with increasing pressure are decreasing errors for a (2.0% \rightarrow 0.0%), increasing errors for b (1.2% \rightarrow 5.3%), and decreasing errors for c (2.7% \rightarrow -0.4%). As was the case for RDX, the lattice angles in β -HMX are accurately predicted. The average values of α and γ (not shown) are 90 ± 0.7 degrees, while the unique angle, β , agrees with experiment to within one degree over the entire pressure domain studied (Table IV).

In Fig. 2, we depict the compression of β -HMX by plotting, as a function of pressure, the ratio V/V^0 of the unit cell volume V at $p \geq 0$ to the $p=0$ value V^0 . The agreement with experiment is good. Although the discrepancy increases with increasing pressure (the error is zero at $p=0$, by definition), at $p=7.47$ GPa, the error in the theoretical prediction for V/V^0 is only -1.8%, i.e., slightly too compressible.

IV. CONCLUSIONS

We have performed Monte Carlo calculations of the isothermal, hydrostatic compression of crystalline RDX and β -HMX, using an all-atom rigid-molecule treatment. Simple potential-energy functions parameterized near ambient conditions were used. Good agreement with published x-ray diffraction data was obtained, suggesting that simulations using potential-energy functions parameterized near ambient con-

ditions can be used to compute the physical properties of polyatomic molecular crystals at elevated pressures. Given the degree of extrapolation involved, it is not obvious that this would be the case; nor is it clear whether this will prove to be true for most crystals. A logical next step is to perform a suite of calculations spanning p - T space and produce a functional form for the quantities computed here, as well as those derivable from them, suitable for use in larger-scale modeling codes. Given the quality of the present results, it also seems reasonable to undertake calculations of the elastic constant matrix and (tensorial) Poisson's ratio for the crystals.

ACKNOWLEDGMENTS

This work was supported by the U.S. Department of Energy, under the auspices of the Los Alamos National Laboratory Explosives Safety Program administered by Philip M. Howe. The author wishes to thank Sam Shaw for useful discussions and a critical reading of the manuscript.

- ¹See, for example, M. K. Spurgeon, Jr. and C. Cerniello, *Arms Control Today* **26**, 15 (1996).
- ²See, for example, *LASL Explosive Property Data*, edited by T. R. Gibbs and A. Popolato (University of California Press, Berkeley, 1980).
- ³W. W. Wood, in *Physics of Simple Fluids*, edited by H. N. V. Temperley, J. S. Rowlinson, and G. S. Rushbrooke (North-Holland, Amsterdam, 1968), Chap. 5, p. 115.
- ⁴M. Parrinello and A. Rahman, *J. Appl. Phys.* **52**, 7182 (1981).
- ⁵S. Yashonath and C. N. R. Rao, *Mol. Phys.* **54**, 245 (1985).
- ⁶D. E. Williams and S. R. Cox, *Acta Crystallogr., Sect. B: Struct. Sci.* **40**, 404 (1984).
- ⁷S. R. Cox, L. Y. Hsu, and D. E. Williams, *Acta Crystallogr., Sect. A: Cryst. Phys., Diff., Theor. Gen. Crystallogr.* **37**, 293 (1981).
- ⁸Gaussian92/DFT, Revision G.1, M. J. Frisch, G. W. Trucks, H. B. Schlegel, P. M. W. Gill, B. G. Johnson, M. W. Wong, J. B. Foresman, M. A. Robb, M. Head-Gordon, E. S. Replogle, R. Gomperts, J. L. Andres, K. Raghavachari, J. S. Binkley, C. Gonzalez, R. L. Martin, D. J. Fox, D. J. Defrees, J. Baker, J. J. P. Stewart, and J. A. Pople, Gaussian, Inc., Pittsburgh, PA, 1993.
- ⁹D. C. Sorescu, B. M. Rice, and D. L. Thompson, *J. Phys. Chem. B* **101**, 798 (1997).
- ¹⁰J. A. Barker and R. O. Watts, *Chem. Phys. Lett.* **3**, 144 (1969).
- ¹¹N. Metropolis, A. W. Rosenbluth, M. N. Rosenbluth, A. H. Teller, and E. Teller, *J. Chem. Phys.* **21**, 1087 (1953).
- ¹²A. Hald, in *Statistical Theory with Engineering Applications* (Wiley, New York, 1952), Chap. 13, p. 338.
- ¹³C. S. Choi and E. Prince, *Acta Crystallogr., Sect. B: Struct. Crystallogr. Cryst. Chem.* **28**, 2857 (1972).
- ¹⁴B. Olinger, B. Roof, and H. Cady, *Symposium International Sur le Comportement Des Milieux Denses Sous Hautes Pressions Dynamiques*, Paris, France, 1978, p. 3.
- ¹⁵C. S. Choi and H. P. Boutin, *Acta Crystallogr., Sect. B: Struct. Crystallogr. Cryst. Chem.* **26**, 1235 (1970).